Sequence Comparison in Reconstruction and Targeting in Underwater Sonar Imaging

Isidora Stanković
GIPSA Lab/Faculty of Electrical Engineering
University Grenoble Alpes/University of Montenegro
Grenoble,France/Podgorica,Montenegro
isidora.stankovic@grenoble-inp.fr

Cornel Ioana
GIPSA Lab, INP Grenoble
University Grenoble Alpes
Grenoble,France
cornel.ioana@grenoble-inp.fr

Miloš Daković
Faculty of Electrical Engineering
University of Montenegro
Podgorica,Montenegro
milos@ucg.ac.me

Abstract—An analysis of different sequences for the reconstruction and targeting of underwater sonar images is presented. The sonar images are assumed to be sparse, and their reconstruction is possible by using the compressive sensing theory. The goal is to localize and reconstruct targets by using an iterative version of the orthogonal matching pursuit (OMP) method. The sequences which are used as the transmitted signal waveforms are formed with: the Alltop sequence, the M sequence, a random Gaussian sequence, a binary random sequence, the Zadoff-Chu sequence, and the Bjorck sequence. The comparison of the reconstruction results is done for various numbers of samples in the sequences and sparsity levels. An analysis of the performance for each of the sequences in various noise levels is done as well. Percentage of successfully detected targets is used as a performance measure.

Index Terms—Comparison, Compressive sensing, Reconstruction, Sequence, Sonar imaging, Sparsity, Targeting

I. INTRODUCTION

The idea of sparse reconstruction from a reduced set of measurements is a well studied topic in the field of signal processing. A signal with very few nonzero samples in one of its representation domains is a sparse signal. When a signal is considered as sparse, it can be reconstructed with a reduced set of measurements. The field dealing with this problem is within the theory of compressive sensing (CS) and sparse signal processing (SSP) [1]–[3]. The idea is to reduce the number of measurements, so that system's processing of the signals (acquisition time, energy, required memory) is also reduced. Other than the desired sampling techniques with reduced set of samples, there are some undesirable constraints that make the signal having a reduced set of measurements. In any case, under certain conditions, the theory of SSP and CS can be used to successfully reconstruct such signals. Since the theory reflects the acquisition of signals, it can be used in many fields and applications. In recent years, many methods and algorithms for the reconstruction and analysis were developed, each corresponding to a specific type of signal. One of the most successful algorithms is the orthogonal matching pursuit (OMP) and its variants [4]–[6].

The radar and sonar signal analysis using CS theory is a topic which has been discussed in the literature. Underwater sonar imaging is a representative example of sparse signal since in a relatively large sonar image there are only a few targets. As such, it may significantly benefit from the compressive sensing techniques. It is confirmed that the CS theory can be used in radar/sonar systems to obtain high-quality images with small amount of measurements. Here, we will consider sonar two-dimensional signals (images) for targeting underwater objects. One of the famous methods for reducing number of measurements in radars, presented in [7], assumes that the radar image is sparse in range-Doppler domain where the targets are represented using the Doppler frequency shifts and delays. The same concept is used in underwater sonar imaging [8]. Although similar, radar and sonar systems have differences which make changes in their configuration and analysis. The sound velocity in sonar systems is much slower than velocity of radar waves, which makes the Doppler frequency shifts spreading over larger spectrum. Besides frequency variation, scaling effect should always be taken into consideration, particularly for the Doppler effect. These changes have to be taken into consideration for a successful application of compressive sensing techniques and signal reconstruction.

In [8], the reconstruction of sonar images using a compressive sensing method and Alltop sequence was examined. In [9], it has been shown that the maximum length sequence (M sequence) can be used for the reconstruction of the sonar images using the basis pursuit algorithm. There exists a vast number of different sequences used for the transmission and analysis of signals, some of them presented in [10]–[17]. In this paper, in addition to the Alltop and M sequences, we will analyze and compare four more sequences, which are: the random Gaussian, the random binary sequences, the Zadoff-Chu, and the Bjorck sequences. The iterative form of the OMP algorithm [6] will be used for sparse signal reconstruction. The comparison will be done for various numbers of available samples, sparsity and noise levels. Percentage of successful target detection (reconstruction of the target component) will be used for comparison. Also, in practice, signals are only approximately sparse due to different reasons such as off-grid effects, noise, background reflection [6], [18]. Reconstruction of approximately sparse images with a sparsity assumption introduces an error in the reconstructed image, which will be analyzed in this paper.

The paper is organized as follows. A general model of sonar

images is described in Section II, together with the definitions of each sequences. The theory of CS and SSP is presented in Section III. The derivation of the exact reconstruction error is introduced in Section IV. The results and comparisons are shown in Section V. Section VI concludes the paper.

II. Sonar Image Modelling

We assume that the sonar image is modelled and calculated using one of six different sequence forms of the transmitted signal. The sequences considered for the signal are: (1) the Alltop sequence, (2) the M sequence, (3) the random Gaussian sequence, (4) the binary random sequence, (5) the Zadoff-Chu sequence (it is shown, that it cannot be used for this sonar image calculation), and (6) the Bjorck sequence.

The general form of the transmitted signal will be denoted by $s(n)$. The transmitted signal is modulated on a carrier frequency f_c. In the continuous time domain, the modulated transmitted signal is of the form [7]–[9]

$$x(t) = s\left(\frac{t}{\Delta}\right) \exp\left(j2\pi f_c t\right), \tag{1}$$

where Δ is the code width of the sequence, $0 \leq t < N\Delta$, and f_c is the carrier frequency.

The echo signal from one point target, with velocity v, is delayed for τ and scaled in frequency due to the Doppler effect for $(c+v)/(c-v)$. The echo signal form is

$$r_1(t) = g\, s\left(\frac{\frac{c+\nu}{c-\nu}(t-\tau)}{\Delta}\right) \exp\left(j2\pi f_c \frac{c+\nu}{c-\nu}(t-\tau)\right), \tag{2}$$

where g is a complex scattering coefficient and c is the speed of sound.

For K scattering points, after demodulation using the carrier frequency f_c, the received discrete echo signal can be written as a sum of K discrete forms of echoes (2) [9], [19], [20]

$$r(n) = \sum_{i=1}^{K} g_{k_i} s(n - d_{k_i}) \exp\left(j\omega_{k_i} n\right), \tag{3}$$

where d_k corresponds to the range (time delay) and ω_k to the cross-range (Doppler shift) of targets. Assume that the range and cross-range coordinates are on the grid and that they may take one of the values from the set

$$(d_p, \omega_q) \in \{d_1, d_2, \ldots d_N\} \times \{\omega_1, \omega_2, \ldots \omega_N\},$$

where

$$\begin{aligned} d_p &\in \{d_1, d_2, \ldots d_N\} \\ \omega_q &\in \{\omega_1, \omega_2, \ldots \omega_N\}. \end{aligned} \tag{4}$$

Note that there are N^2 possible target positions in total. This model is applicable for real target positions as well. Then an off-grid target will spread over a few grid points. The off-grid effects are analyzed in [6].

The received echo, with the assumed discrete grid for the range and cross-range, can be written as

$$r(n) = \sum_{i=1}^{K} g_{k_i} \phi_{k_i}(n), \tag{5}$$

where $\phi_k(n)$ are the basis functions defined by

$$\phi_k(n) = s(n - d_k) \exp\left(j\omega_k n\right). \tag{6}$$

The basis function for a given pair $(d_p, \omega_q) = (p, \frac{2\pi}{N}q)$, corresponding to the scatterer k, can be written as

$$\phi_{p,q}(n) = s(n - p) \exp\left(j2\pi q \frac{n}{N}\right) \tag{7}$$

and

$$r(n) = \sum_{i=1}^{K} g_{k_i} \phi_{p_i, q_i}(n). \tag{8}$$

The scatterer index k and the indices of its range position p and cross-range position q are related as

$$\begin{aligned} k &= p + Nq, \\ p &= k - N\lfloor k/N \rfloor \\ q &= \lfloor k/N \rfloor \end{aligned}$$

with $p = 0, 1, \ldots, N-1$, $q = 0, 1, \ldots, N-1$, and $k = 1, 2, \ldots, N^2 - 1$ and $\lfloor k/N \rfloor$ is the rounding of k/N to the first lower integer value.

The periodic autocorrelation of the signal $s(n)$ is defined by

$$R_s(n) = \sum_{m=1}^{N} s(n + m)s^*(m). \tag{9}$$

This function is closely related to the coherence index,

$$\mu = \max_{k,p} \frac{|\sum_n \phi_k(n)\phi_p^*(n)|}{\sqrt{\sum_n |\phi_k(n)|^2}\sqrt{\sum_n |\phi_p(n)|^2}},$$

as a very important parameter in the compressive sensing [3].

Next, we will consider and compare various sequences that can be used in the sonar image modelling and implementation.

A. Alltop sequence

The transmitted signal can be formed using the Alltop sequence as its $s(n)$ part, [6]–[8]. This sequence can be written as

$$s(n) = \frac{1}{\sqrt{N}} e^{j2\pi \frac{n^3}{N}} \tag{10}$$

where $0 \leq n \leq N-1$. The Alltop sequence, for $N = 31$, is shown in Fig. 1(a), along with its periodic auto-correlation function $R_{ss}(n)$.

The property of this sequence, important for this application is that the side lobes of the auto-correlation function are small. Indeed, for the Alltop sequence the side lobes are of $1/\sqrt{L}$ order for the periodic auto-correlation function. The side lobes remain close to this value for the aperiodic auto-correlation function as well.
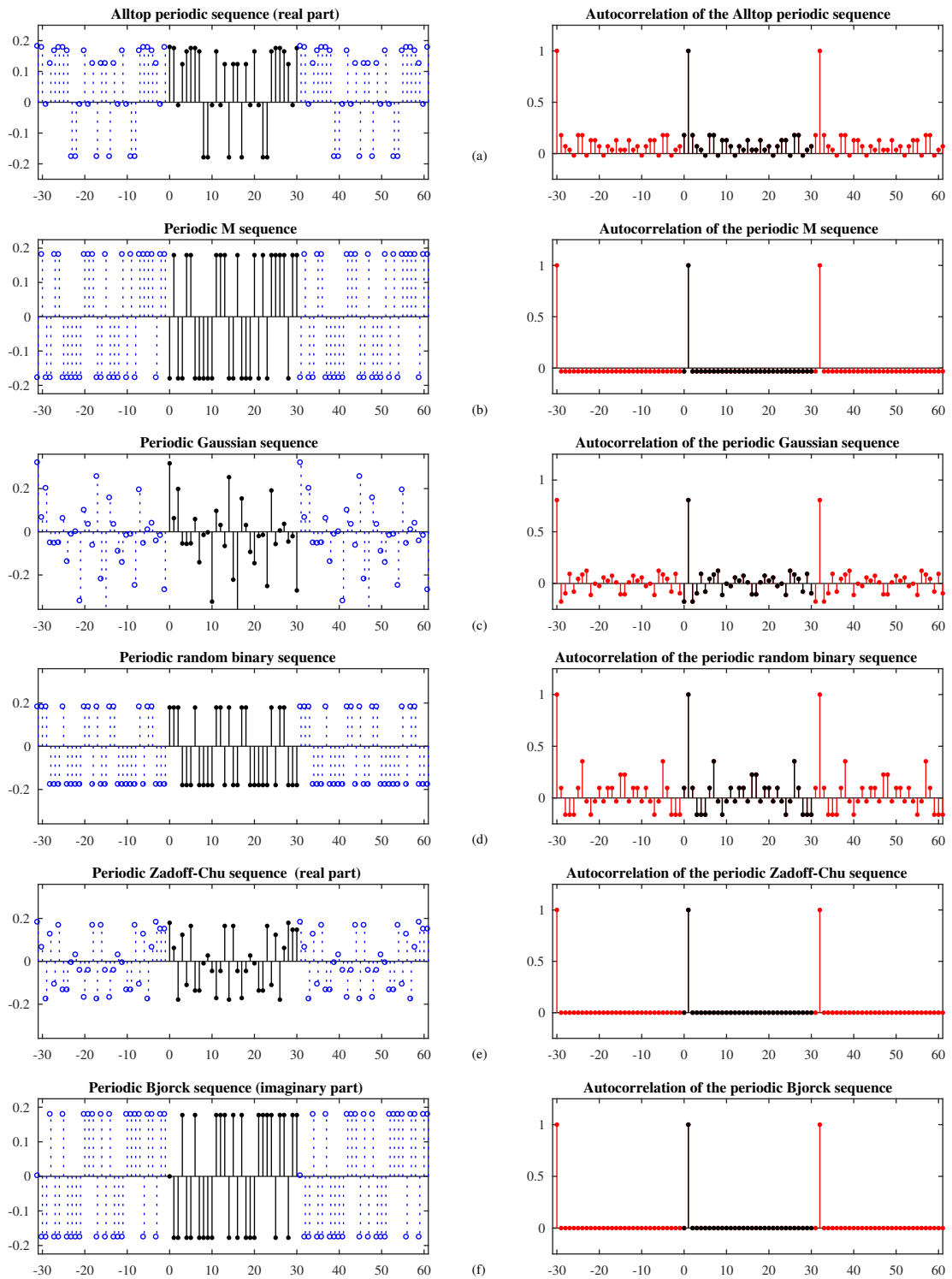
Fig. 1. Various sequences (left) and their autocorrelation functions (right)

B. M sequence

The M sequence (or maximum length sequence - MLS) is a pseudo-random binary sequence based on linear feedback shift register sequences. This pseudo-random sequence is widely used in many systems, including digital communication systems that employ direct-sequence spread spectrum and frequency-hopping spread spectrum transmission systems.

The sequence is generated using the recursive formula [9], [10]

$$s(n) = \sum_{m=1}^{N} c_m s(n - m) \qquad (11)$$

The M sequence is normalized so that its energy in N samples is equal to one. The number of occurrences of values $-1/\sqrt{N}$ and $1/\sqrt{N}$ in the M sequence are approximately the same. For the sequence of length $N = 2^m - 1$ the number of $1/\sqrt{N}$s is $N/2$, while the number of $-1/\sqrt{N}$s is $N = N/2 - 1$. An example of the M sequence, for $N = 31$ is presented in Fig. 1(b).

Property of the M sequence is that its periodic auto-correlation function is of the form

$$R_s(n) = \begin{cases} 1, & \text{for } n = kN \\ -1/N, & \text{elsewhere} \end{cases} \qquad (12)$$

The periodic auto-correlation function for the M sequence and $N = 31$ is given in Fig. 1(b).

For the compressive sensing it is important to notice that the measurement matrices formed from the M sequences are characterized by almost the same coherence index as the Alltop sequences.

C. Random Gaussian sequence

In the case of Gaussian random sequence the signal $s(n)$ assumes the values distributed according to the zero-mean and unit variance normal Gaussian form

$$s(n) \sim \frac{1}{\sqrt{N}} \mathcal{N}(0, 1). \qquad (13)$$

The auto-correlation function of this random signal is

$$R_s(n) = \mathrm{E}\{s(n + m)s(m)\} = \delta(n - m). \qquad (14)$$

Note that for limited sequence the auto-correlation function is just an approximation of this form. One random realization of the Gaussian form of the signal $s(n)$ and its periodic auto-correlation function are show in Fig. 1(c).

D. Random binary sequence

The random sequence that randomly assumes values $1/\sqrt{N}$ and $-1/\sqrt{N}$, with equal probability may be used as a signal $s(n)$. A random realization of this signal and its periodic autocorrelation function, for $N = 31$ are given in Fig. 1(d).

E. Zadoff-Chu sequence

The Zadoff-Chu sequence is defined as [13], [14]

$$s_\gamma(n) = \begin{cases} \frac{1}{\sqrt{N}} \exp\left(-j\frac{2\pi\gamma}{N}\frac{n(n+2Q)}{2}\right), & N \text{ even}, \\ \frac{1}{\sqrt{N}} \exp\left(-j\frac{2\pi\gamma}{N}\frac{n(n+1+2Q)}{2}\right), & N \text{ odd}. \end{cases} \qquad (15)$$

where γ is integer such that $\gcd(\gamma, N) = 1$ and Q is arbitrary integer.

This sequence had the auto-correlation function

$$R_s(n) = \sum_{m=1}^{N} s(n + m)s^*(m) = \delta(n - m). \qquad (16)$$

This is an interesting an important property that would highly recommend this sequence.

The Zadoff-Chu sequence is a constant amplitude zero autocorrelation (CAZAC) sequence, since it has almost zero size lobes of the periodic auto-correlation function [15], [16].

However, if we take into account that this auto-correlation is multiplied by the other part in the received signal, then the ambiguity for the range and cross-range appears. It can not be resolved, making this sequence unsuitable for the sonar imaging applications. The Zadoff-Chu sequence and its autocorrelation functions are shown in Fig. 1(e), for $N = 31$.

F. Bjorck sequence

The Bjorck sequence is defined by [17]

$$s(n) = \frac{1}{\sqrt{N}} \exp\left(j[(n/N)]\arccos(\frac{1}{1 + \sqrt{N}})\right),$$
$$n = 0, 1, \dots, N - 1,$$

where N is a prime number that assumes the form $N = 4m + 1$ and $[(n/N)]$ is the Legendre symbol that takes values ± 1 and 0 as

$$[(n/N)] = \begin{cases} 0, & \text{for } n = 0 \bmod N \\ +1, & \text{for } n \text{ is a qudratic residue } mod \ N \\ -1, & \text{for } n \text{ is a qudratic nonresidue } mod \ N \end{cases}$$

The Bjorck sequence is also a CAZAC sequence, since it has almost zero size lobes of the periodic auto-correlation function [15], [16]. The Bjorck sequence and its autocorrelation functions are shown in Fig. 1(f), for $N = 33$.

III. Sparse Signal Processing

Any considered sequence can be used to define the measurement matrix and fit into the framework of compressive sensing theory and sparse signal processing. We can rewrite the samples of received signal, defined by (8), in a matrix from

$$\mathbf{r} = \mathbf{\Phi}\mathbf{g}, \qquad (17)$$

where $\mathbf{r}$ is the column vector of the echo signal, $\mathbf{\Phi}$ is the basis functions matrix and $\mathbf{g} = [g(0), g(1), \dots, g(N^2 - 1)]^T$ is the column vector of the scattering coefficients $g(k) = g_k$.

TABLE I
ELEMENTS OF THE THE FUNCTION $s(n)$ FROM EQ. (20)

Sequence	Elements
Alltop	$\frac{1}{\sqrt{N}} \exp\left(2\pi j n^3/N\right)$
M sequence	$\frac{1}{\sqrt{N}} \text{MLS}\{2^\gamma - 1\}$
Gaussian	$\sim \frac{1}{\sqrt{N}} \mathcal{N}(0,1)$
binary	$\sim \frac{1}{\sqrt{N}} \text{sign}(\mathcal{N}(0,1))$
Zadoff-Chu	$\frac{1}{\sqrt{N}} \exp\left(-j\frac{2\pi\gamma n}{N}(n + 2Q + \text{mod}(N,2))\right)$
Bjorck	$\frac{1}{\sqrt{N}} \exp\left(j[(n/N)]\arccos(\frac{1}{1+\sqrt{N}})\right)$

The scattering vector $\mathbf{g}$ is assumed to be K-sparse since the echo is produced by only K reflecting points, and this number is assumed to be much smaller than the total number of possible scattering points $N \times N$.

Since of the vector $\mathbf{g}$ is sparse then, according to the compressive sensing theory, all its values can be reconstructed from a reduced set of the received signal samples [1]–[3], considered as observations $\mathbf{y}$,

$$\mathbf{y} = [r(n_1), r(n_2), \ldots, r(n_M)]^T \qquad (18)$$

or

$$\mathbf{y} = \mathbf{A}\mathbf{g} \qquad (19)$$

where the measurement matrix $\mathbf{A}$ is obtained from the full matrix $\boldsymbol{\Phi}$ by keeping the rows corresponding to the available samples at $n_i \in \mathbb{M} = \{n_1, n_2, \ldots, n_M\}$. The elements of the measurement matrix are defined as in (7)

$$a_{k,l} = s(n_l - d_p) \exp\left(j\omega_q n_l\right), \qquad (20)$$

where d_p and ω_q correspond to the vector rearranged coefficients (range and cross-range) for a given scattering position, denoted by index k. As mentioned, the function $s(n - p)$ is defined by one of the listed sequences, which will be used in particular applications. The elements of $s(n)$ are summed up in Table I.

The task of a compressive sensing reconstruction is to produce all values of $\mathbf{g}$, by minimizing its number of nonzero samples, that is equal to $\|\mathbf{g}\|_0$, subject to the given values of the received signal given in $\mathbf{y}$ [1]–[3]. It can be written as a general compressive sensing problem formulation

$$\min \|\mathbf{g}\|_0 \text{ subject to } \mathbf{y} = \mathbf{A}\mathbf{g}. \qquad (21)$$

In other words, the aim is to reconstruct the sparsest possible reflection coefficients vector $\mathbf{g}$, by minimizing the number of its nonzero elements $\|\mathbf{g}\|_0$ subject to the available samples $\mathbf{y}$. There are several approaches, with various methods within each of them, to solve this problem. The most important approaches are based on the components matching pursuit, convex relaxation of the minimization problem and gradient based-algorithms to find the solution, and the Bayesian based formulations and reconstruction. A simple reconstruction method [6], that belongs to the components matching pursuit, will be used in this paper.

A. Initial estimate

For the reconstruction of sparse signal $\mathbf{g}$, we will use its initial estimate as a projection of the available measurements of the received echo on the measurement matrix. The initial estimate is calculated by using the available samples [21], [22]

$$\mathbf{g}_0 = \mathbf{A}^H \mathbf{y} \qquad (22)$$

or

$$g_0(k) = \sum_{n_i \in \mathbb{M}} r(n_i) a_{k,n_i}^*. \qquad (23)$$

If we replace the echo signal we get

$$g_0(k) = \sum_{n_i \in \mathbb{M}} \sum_{i=1}^{K} g_{k_i} \phi_{p_i, q_i}(n_i) a_{k,n_i}^*. \qquad (24)$$

We will denote the terms $\sum_{n_i \in \mathbb{M}} \phi_{p_i, q_i}(n_i) a_{k,n_i}^*$ by $\mu(k, k_i)$ we get

$$\mu(k, k_i) = \sum_{n_i \in \mathbb{M}} \phi_{p_i, q_i}(n_i) a_{k,n_i}^*$$

$$= \sum_{n_i \in \mathbb{M}} s(n_i - d_k) s^*(n_i - p_i) e^{j2\pi(q_i - q)n_i/N}$$

and

$$g_0(k) = \sum_{i=1}^{K} g_{k_i} \mu(k, k_i). \qquad (25)$$

Note that, with a random set of available samples, the value of $\mu(k, k_i)$ and the initial estimate $g_0(k)$ are random variables [18], [22]. When the summation over n_i is performed over all indices $n_i = 0, 1, 2, \ldots, N - 1$, then

$$\mu(k, k_i) = \sum_{n=0}^{N-1} s(n - d_k) s^*(n - p_i) e^{j2\pi(q_i - q)n/N}.$$

Note that taking all samples $n_i = 0, 1, 2, \ldots, N - 1$, we still have case of the reduced number of samples and the need for the CS based reconstruction since the number of possible target positions is $N \times N = N^2 \gg M = N$.

The maximal absolute value of $\mu(k, k_i)$, for $k \neq k_i$, is called the coherence index of the measurement matrix $\mathbf{A}$. It defines the condition for the unique reconstruction of a sparse signal from a reduced set of sample [1]–[3], [21]. The uniqueness condition is $K < (1 + 1/\mu)/2$. It can be easily derived from the analysis of the initial estimate.

In the case of $n_i = 0, 1, 2, \ldots, N - 1$, the analysis of the maximal absolute value of term $\mu(k, k_i)$ for $q_{k_i} = q_k$ reduces to the analysis of the autocorrelation function

$$\mu(k, k_i) = \sum_{n=0}^{N-1} s(n - d_k) s^*(n - p_i), \text{ for } q_i = q.$$

This means that we may expect good performance in the compressive sensing reconstruction when the maximum absolute value of side lobes of the autocorrelation function $|\sum_{n=0}^{N-1} s(n - d_k) s^*(n - p_i)|$ are minimized (for $d_k \neq p_i$). Although the coherence index is very pessimistic, it can be a

good indicator the reconstruction quality that we may expect from the presented sequences.

However, in general, we should consider the whole expression for $\mu(k, k_i)$ and $k \neq k_i$. It reduces to the analysis of

$$AF(n, r) = \sum_{m=0}^{N-1} s(n+m)s^*(m)e^{j2\pi rm/N},$$

for all n and r. This form is equal to the ambiguity function of the Rihaczek distribution of the sequence. The analysis of coherence index reduces then to the calculation of the maximum value of $|AF(n,r)|$ for $(n,r) \neq (0,0)$. Note that $AF(0,0) = \mu(k,k) = 1$.

The ambiguity functions (their absolute values) of the considered sequences are presented in Fig. 2. It is obvious that Zadoff-Chu sequence can not be used, since it produces values $AF(m,r) = 1$ for $(m,r) \neq (0,0)$.

The mean and the variance of $\mathbf{g}_0$ are calculated using the randomly sampled available signal measurements [18]. The one-target initial estimate is calculated as

$$g_0(k) = \sum_{n_i \in \mathbb{M}} g_{k_1} \phi_{p_1,q_1}(n_i) a^*_{k,n_i}.$$

When the position is found, i.e. $k = k_1$, its mean is $E\{g_0(k)\} = g_{k_1} M/N$. Since $\mathbb{M}$ is a random set, for $k \neq k_1$ the initial estimate behaves as random variable with zero-mean and variance $\text{var}\{g_0(k)\} = |g_{k_1}|^2 M/N^2$. Now the results can easily be generalized for any sparsity K

$$E\{g_0(k)\} = \sum_{i=1}^{K} \frac{M}{N} g_{k_i} \delta(k - k_i) \tag{26}$$

$$\text{var}\{g_0(k)\} = \frac{M}{N^2} \sum_{i=1}^{K} |g_{k_i}|^2 (1 - \delta(k - k_i)), \tag{27}$$

where $\delta(k) = 1$ only for $k = 0$ and $\delta(k) = 0$, elsewhere.

IV. ERROR CALCULATION FOR NONSPARSE IMAGES

In real data, signals are only approximately sparse or nonsparse. This can happen for many reasons, such as noisy measurements or off-grid sampling [18]–[20]. Let consider a reflected echo signal $\mathbf{r}$ that is only approximately sparse in the coefficients $\mathbf{g}$ domain. When the signal is not strictly sparse, it has more non-zero components in the representation domain. However, in order to use the theory of CS, the sparsity assumption has to be made. The error which is produced by the reconstruction of nonsparse signal with such assumption is calculated in this paper. We will assume that the CS conditions for the reconstruction are satisfied with assumed sparsity K and the number of available samples M, so that we can detect and reconstruct K components of $\mathbf{g}$.

The reconstructed coefficients vector has K (nonzero) reconstructed components, meaning that $N^2 - K$ coefficients remained unreconstructed. Following (27), one unreconstructed coefficients produces noise in the reconstructed components with variance $|g_i|^2 M/N^2$. The noise variance in the reconstructed coefficients will have a scaling factor of $(N/M)^2$,

since the signal amplitudes in the initial estimate are proportional to M and the amplitudes are recovered to their original values as if all samples were available, proportional to its size. Therefore, the variance of noise which causes a single reflection coefficients which is not reconstructed to the reconstructed one is $|g_i|^2 \frac{M}{N^2} \left(\frac{N}{M}\right)^2 = \frac{1}{M} |g_i|^2$.

For a signal reflected from K points, the noise energy in the reconstructed coefficients will be K times larger than the energy (variance) in one reconstructed coefficient. Then, the total noise energy caused by the unreconstructed coefficients can be written as

$$\|\mathbf{g}_R - \mathbf{g}_K\|_2^2 = \frac{K}{M} \sum_{i=K+1}^{N^2} |g_i|^2. \tag{28}$$

Energy corresponding to the unreconstructed $N - K$ coefficients is obviously

$$\|\mathbf{g} - \mathbf{g}_K\|_2^2 = \sum_{i=K+1}^{N^2} |g_i|^2. \tag{29}$$

Finally, combining (28) and (29), we can conclude that the error in the reconstructed coefficients with respect to the K corresponding coefficients if the original signal were used is

$$\|\mathbf{g}_R - \mathbf{g}_K\|_2^2 = \frac{K}{M} \|\mathbf{g} - \mathbf{g}_K\|_2^2, \tag{30}$$

where $\|\mathbf{g}\|_2^2 = E\{\sum_k |g(k)|^2\}$ is the expected value of squared norm-two, $\mathbf{g}_K$ is the K-sparse version of $\mathbf{g}$. The elements of vector $\mathbf{g}_K$ are $g_K(k) = g(k)$ for $k \in \mathbb{K}$, and $g_K(k) = 0$ for $k \notin \mathbb{K}$. The reconstructed vector $\mathbf{g}_R$ is formed in the same way. The coefficients at $k \in \mathbb{K}$ are the results from the reconstruction procedure and $g_R(k) = 0$ at $k \notin \mathbb{K}$.

The case without noise is considered as the ideal case. In real scenarios, the received signals have some noise. Having noisy available measurements i.e.

$$\mathbf{y}_n + \boldsymbol{\varepsilon}_n = \mathbf{A}\mathbf{g}. \tag{31}$$

will result in a noisy initial estimate $g_0(k)$

$$g_0(k) = \sum_{n_i \in \mathbb{M}} (r(n_i) + \varepsilon(n_i)) a^*_{k,n_i}.$$

The variance of additive noise ε is σ_ε^2. Additive noise caused variance in each term is σ_ε^2/N. Then the total initial estimate variance is $\sigma_{g_0(k)}^2 = M\sigma_\varepsilon^2/N$. Since the initial estimate is multiplied by N/M in the reconstruction, the noise variance in the reconstructed component is $\sigma_\varepsilon^2 N/M$ [6], [18].

The total error in K reconstructed coefficients is

$$\|\mathbf{g}_R - \mathbf{g}_K\|_2^2 = K \frac{N}{M} \sigma_\varepsilon^2. \tag{32}$$

In general case, when the signal is approximately sparse and noisy, the error will then be calculated as [6], [18]

$$\|\mathbf{g}_R - \mathbf{g}_K\|_2^2 = \frac{K}{M} \|\mathbf{g} - \mathbf{g}_K\|_2^2 + K \frac{N}{M} \sigma_\varepsilon^2. \tag{33}$$
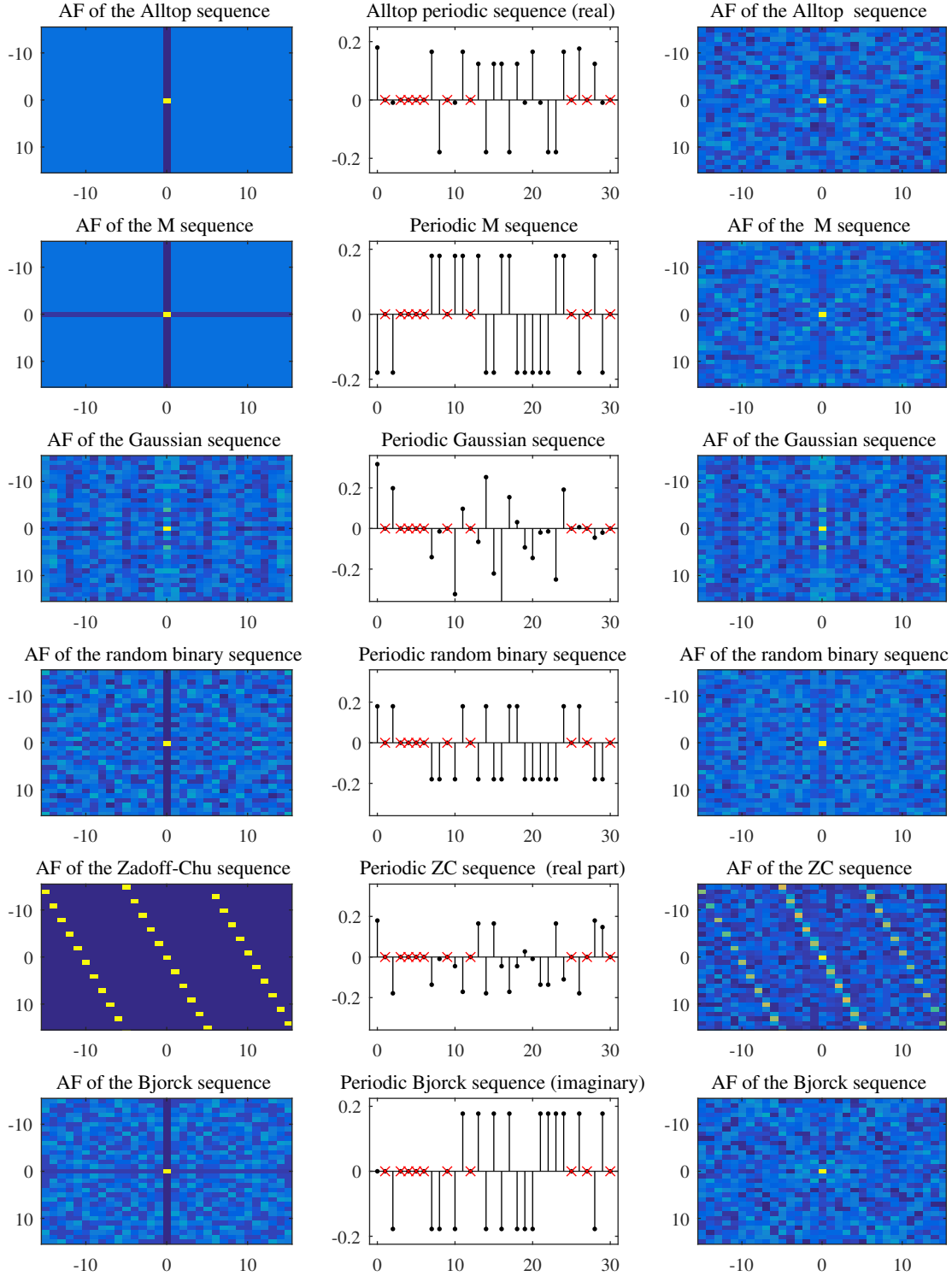
Fig. 2. Various sequences and the inner products of the columns of the full measurement matrix for various target indices k, corresponding to their ambiguity functions of the Rihaczek distributions (AF), with full form of sequences $s(n)$ with $M = N = 31$ (left). The sequences with missing samples, when $M = 21$ samples are available, out of $N = 31$ (middle). Inner products of the columns of the measurement matrix for various target indices k with missing samples in sequences (right). The coherence index is equal to the maximum value at $(n, r) \neq (0, 0)$.
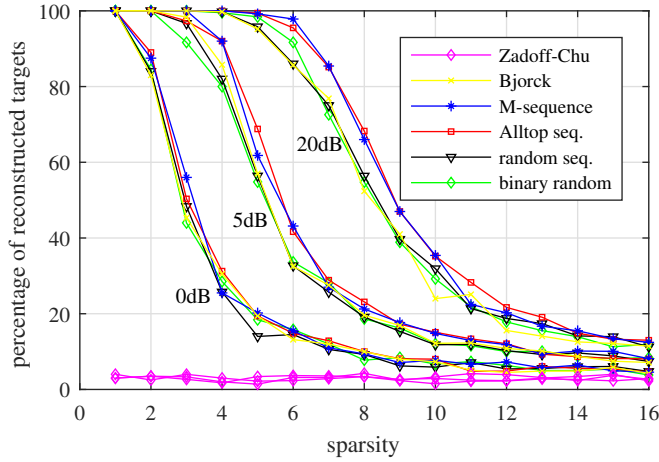
Fig. 3. Target detection rate for various sparsity levels and signal to noise ratios for the considered sequences

V. RESULTS

Example 1: Percentage of found targets. In this example, we will statistically analyze how each sequence behaves in various environments. We consider a sparse signal with various sparsity levels, varying from 0 until 16. The considered SNR values are 20dB, 5dB, and 0dB. The average reconstruction success in terms of percentage of reconstructed targets in 100 realizations of each sequence is calculated. Results for $N = 31$ for all analyzed sequences and varying sparsity level are shown in Fig. 3. It is seen that, in low noise environments, the Alltop and M sequence have the best performance. In high noise environments, the Bjorck sequence can also compete with them. The Gaussian and binary random sequence show satisfactory results. The Zadoff-Chu, as expected, failed to detect targets in any case.

Example 2: Error calculation. The error calculation for the nonsparse and noisy cases are shown in this example. The statistical and theoretical error, respectively, are calculated as

$$E_s = 10\log\left(\|\mathbf{g}-\mathbf{g}_R\|_2^2\right), \tag{34}$$

$$E_t = 10\log\left((\frac{K}{M}+1)\|\mathbf{g}-\mathbf{g}_K\|_2^2 + K\frac{N}{M}\sigma_\varepsilon^2\right). \tag{35}$$

The average of 1000 realizations is taken, since we ignored the cases when we could not find the right positions of the targets. The results for SNR=20dB and SNR=5dB are shown in Table II. Although the M sequence is the best for finding the targets, it is seen that, in the cases when the positions are successfully found, the Alltop sequence shows slightly better results in the reconstruction. Also note that the theoretical and statistical error give almost identical values in all considered cases.

Example 3: Analysis of the number of available samples on the best sequences. From Example 1 we see that the sequences M, Alltop and Bjorck show the most reliable results in terms of the percentage of found targets. In this example, we will further examine those sequences. Target detection rate,
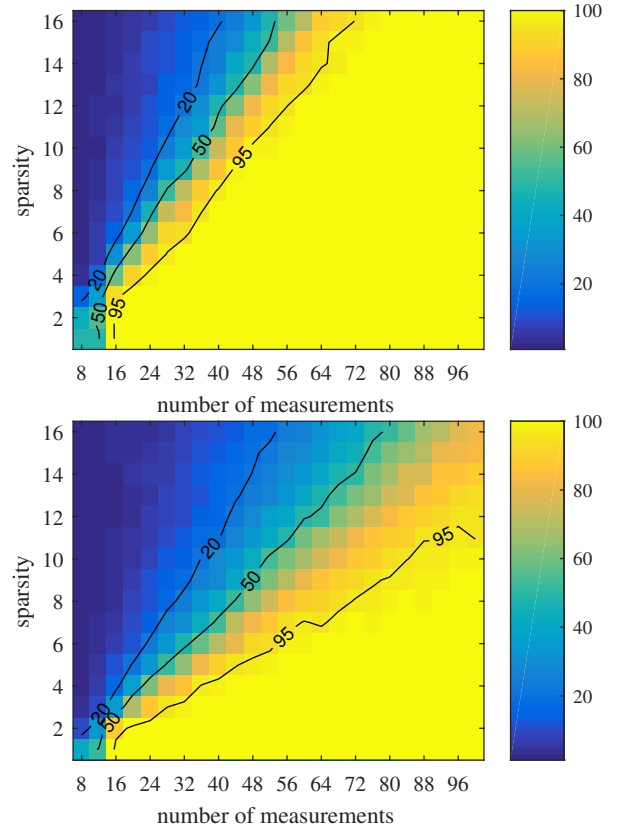

Fig. 4. Successful reconstruction percentage for M sequence for $SNR = 20$dB (top) and $SNR = 5$dB (bottom)

in terms of different number of sparsity levels and various number of measurements, using the M sequence, is shown in Fig. 4 for a high and moderate signal to noise ratio. The same for Alltop sequence is shown in Fig. 5 and in Fig. 6 for the Bjorck sequence. We can see that the M sequence and the Bjorck sequence are more robust to changing the number of measurements than the Alltop sequence.

Example 4: The best sequences on randomly positioned targets. After the deep analysis on different sequences, the sequences M and Bjorck are used for the final reconstruction of data. We will consider an area of interest with 5 targets randomly positioned and more targets which arrived due to noise or off-grid sampling. We consider a noisy case with SNR=10 dB. The original area of interest is shown in Fig. 7 (top). The reconstruction using the Bjorck sequence and the M-sequence is shown in Fig. 7 (middle, bottom), respectively.

Example 5: The best sequences on a set-up data. In Fig. 8 (top) a set-up of a boat under water is modelled. In this case, the number of our target depends on the number of points with which the boat is analyzed. In Fig. 8 (top), the number is $K = 14$. Since the number of targets is high, the sequences are considered with $N = 127$. It is also assumed that noise exists with SNR=15 dB. The reconstruction with the M sequence is shown in Fig. 8 (middle) and the reconstruction with the Bjorck sequence is shown in Fig. 8 (bottom).

SNR= 20dB	M seq.	Alltop	Bjorck	Gaussian	Binary	Zadoff-Chu
Statistics	−10.55	−10.52	−9.37	−9.22	−9.36	0.02
Theory	−10.60	−10.66	−9.51	−9.18	−9.42	0.00
SNR= 5dB	M seq.	Alltop	Bjorck	Gaussian	Binary	Zadoff-Chu
Statistics	−1.26	−1.03	−0.60	−0.74	−0.90	0.01
Theory	−1.23	−1.31	−0.75	−0.63	−0.90	0.00
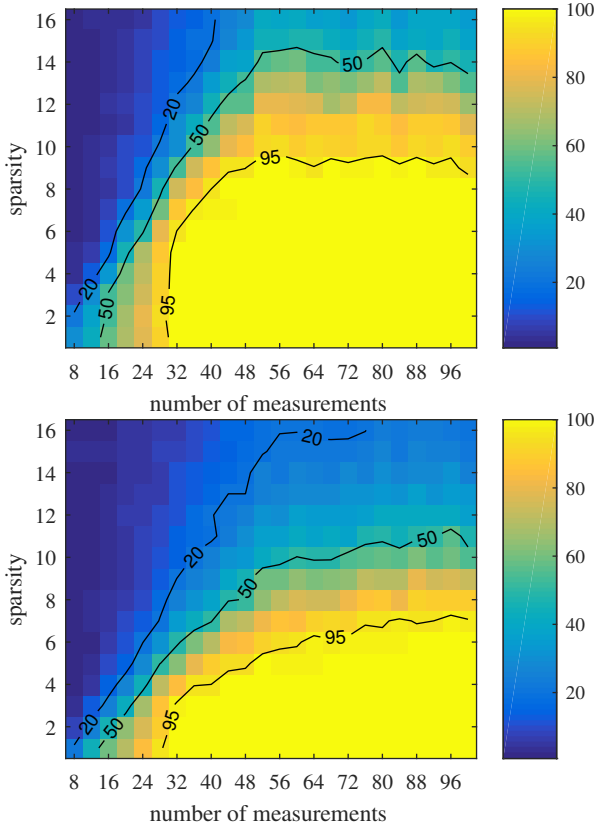
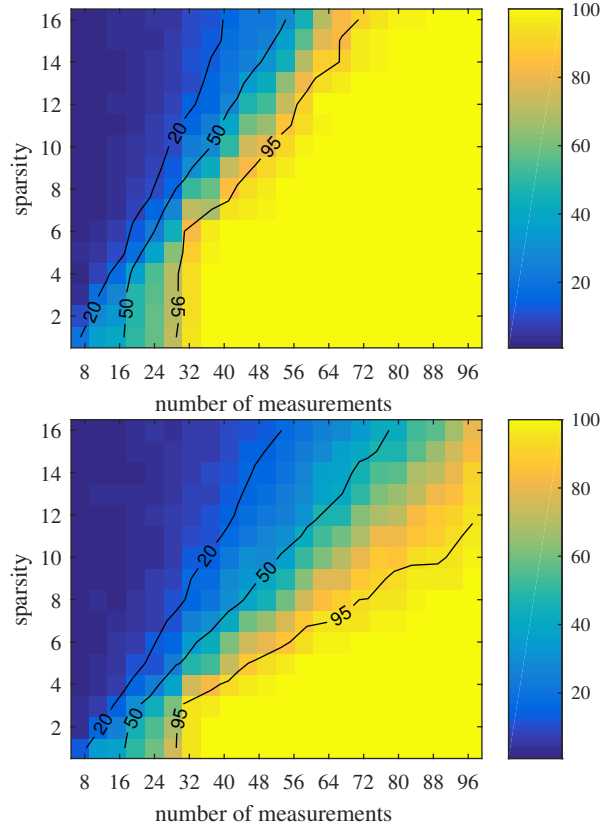Fig. 5. Successful reconstruction percentage for Alltop sequence for $SNR = $ 20dB (top) and $SNR = $ 5dB (bottom)

Fig. 6. Successful reconstruction percentage for Bjorck sequence for $SNR = $ 20dB (top) and $SNR = $ 5dB (bottom)

VI. CONCLUSIONS

The comparison of sequences for the reconstruction and targeting of underwater sonar images is analyzed. It is assumed that the images are sparse, and their reconstruction is possible by using the compressive sensing theory. Then, the goal is to localize and reconstruct the target by using an iterative variant of the OMP method. The comparison is performed for various number of available samples and sparsity levels, as well as different noise levels. It is seen that the Bjorck and M sequence over-perform randomly generated sequences (Gaussian and binary) in low noise setups. The Alltop sequence showed good results also. It is shown that the Zadoff-Chu sequence cannot be used because of its quadratic behaviour. Future work will consider gathering and reconstruction of real data to successfully detect all targets.

REFERENCES

[1] R. G. Baraniuk, "Compressive sensing," *IEEE Signal Processing Magazine*, vol. 24, no. 4, pp. 118–121, 2007.

[2] D. L. Donoho, "Compressed sensing," *IEEE Trans. Information Theory*, vol. 52, no. 4, pp. 1289–1306, 2006.

[3] E. J. Candès and M. B. Wakin, "An Introduction to Compressive Sampling," *IEEE Signal Processing Magazine*, vol. 21, March 2008.

[4] D.Needell, and J.A.Tropp, "CoSaMP: Iterative signal recovery from incomplete and inaccurate samples,"*Applied and Computational Harmonic Analysis*, vol. 20, no. 3, pp. 301?321, May 2009.

[5] I. Stanković, C. Ioana, and M. Daković, "On the reconstruction of nonsparse time-frequency signals with sparsity constraint from a reduced set of samples,"*Signal Processing*, vol. 142, pp. 480-484, January 2018.

[6] I. Stanković, C. Ioana, M. Daković, and L. Stanković, "Analysis of off-grid effects in wideband sonar images using compressive sensing," *IEEE OCEANS 2018*, Charleston, South Carolina, USA, October 2018.

[7] M. A. Herman and T. Strohmer, "High-resolution radar via compressed sensing," *IEEE Transactions on Signal Processing*, vol. 57, no. 6, pp. 2275–2284, Jun 2009.
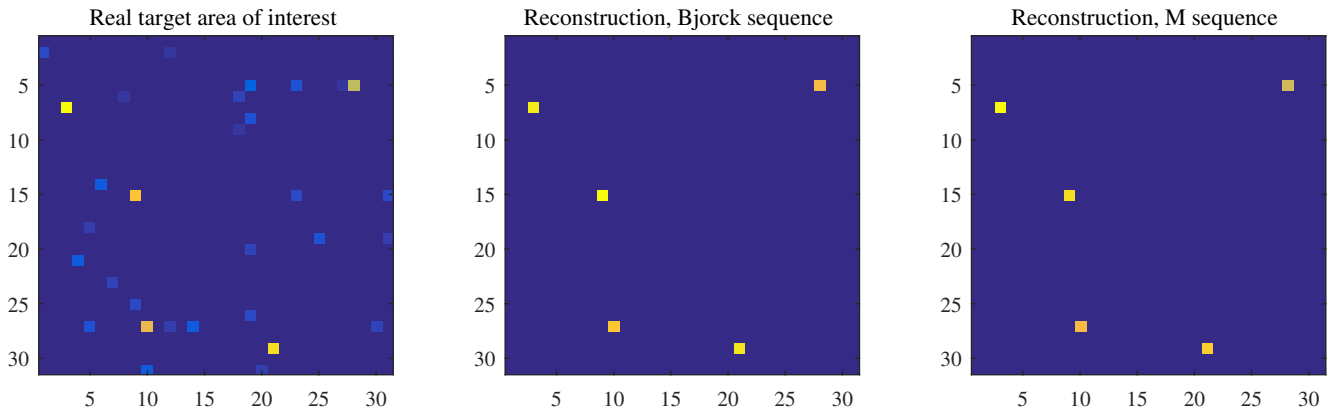
Fig. 7. The reconstruction of a nonsparse and noisy area with $SNR = 10$dB and $K = 5$: area of interest (left), reconstruction with Bjorck (middle) and M sequence (right)
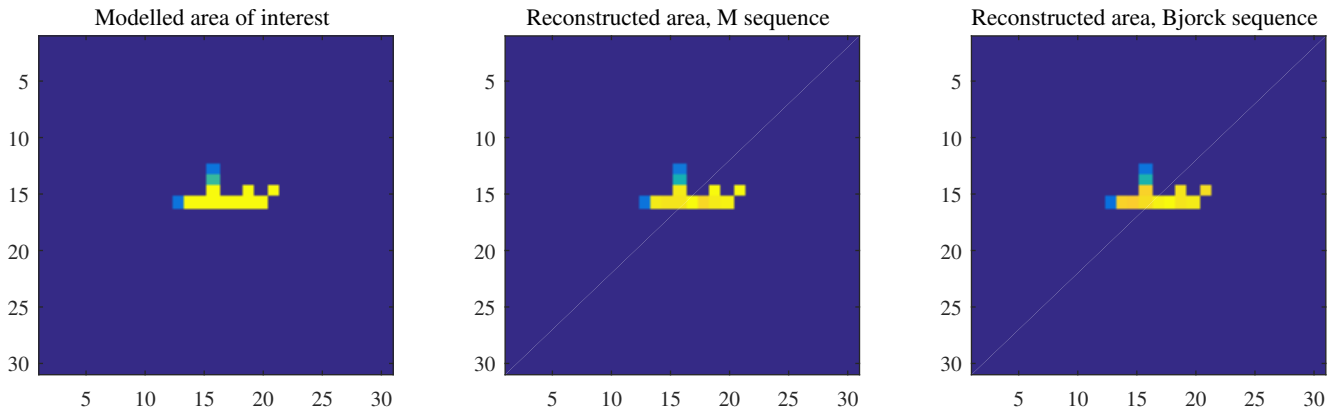

Fig. 8. The reconstruction of a noisy area with a simulated target boat with $SNR = 15$dB (left): area of interest (left), reconstruction with M sequence (middle) and Bjorck sequence (right)

[8] H. Yan, S. Peng, Z. Zhu, J. Xu, and X. Zhang, "Wideband sonar imaging via compressed sensing," *IEEE OCEANS 2014*, Taipei, Taiwan, November 2014.

[9] H. Yan, J. Xu, X. Xia, X. Zhang, and T. Long, "Underwater sonar target imaging via compressed sensing with M sequences," *Science China Information Sciences*, vol. 59, no. 12, December 2016.

[10] Dinan E, Jabbari B. Spreading codes for direct sequence CDMA and wideband CDMA cellular networks. IEEE Commun Mag, 1998, 36: 48-54

[11] S. Sajic, N. Maletic, B. Todorovic, M. Sunjeravic, "Random Binary Sequences in Telecommunications," *Journal of Electrical Engineering*, vol. 64, no. 4, pp. 230 - 237, 2013.

[12] A. Mitra "On Pseudo-Random and Orthogonal Binary Spreading Sequences," *International Journal of Information Technology*, vol. 4, no. 2, pp. 137 - 144, 2007.

[13] D. C. Chu, "Polyphase codes with good periodic correlation properties," *IEEE Trans. on Inf. Theory*, vol. IT-18, pp. 531?532, Jul. 1972.

[14] K. Li, L. Gan, and C. Ling, "Convolutional compressed sensing using deterministic sequences," *IEEE Transactions on Signal Processing*, vol. 61, no. 3, pp. 740-752, February 2013.

[15] J. Bendetto, J. Donatelli, "Ambiguity Function and Frame-Theoretic Properties of Periodic Zero-Autocorrelation Waveforms," *IEEE Journal of Selected Topics in Signal Processing*, vol. 1, no. 1, pp. 6-20, July 2007.

[16] A. Kebo, I. Konstanidinidis, J. Bendetto, M. Dellomo, and J. Sieracki "Ambiguity and sidelobe behavior of CAZAC coded waveforms," *IEEE Radar Conference*, Boston, MA, USA, April 2007.

[17] G. Björck, "Functions of modulus one on Zn whose Fourier transforms have constant modulus, and cyclic n-roots," *In: Byrnes J.S., Byrnes J.L. (eds) Recent Advances in Fourier Analysis and Its Applications. NATO ASI Series (Series C: Mathematical and Physical Sciences)*, vol 315. Springer, Dordrecht, pp. 131-140., 1990.

[18] L. Stanković, M. Daković, I. Stanković, and S. Vujović, "On the Errors in Randomly Sampled Nonsparse Signals Reconstructed With a Sparsity Assumption," *IEEE Geoscience and Remote Sensing Letters*, vol. 14, no. 12, pp. 2453–2456, Dec. 2017.

[19] H. Yan, J. Xu, X. Zhang, "Compressed Sensing Radar Imaging of off-grid sparse targets," *IEEE Radar Conference RadarCon*, 2015.

[20] H. Yan, J. Xu, et al. "Wideband underwater sonar imaging via compressed sensing with scaling effect compensation," *Science China*, February 2015, Vol. doi: 10.1007/s11432-014-5264-8

[21] E. J. Candes, J. Romberg, and T. Tao, "Robust uncertainty principles: exact signal reconstruction from highly incomplete frequency information," *IEEE Transactions on Information Theory*, vol. 52, no. 2, pp. 489–509, Feb. 2006.

[22] L. Stanković, S. Stanković, and M. G. Amin, "Missing samples analysis in signals for applications to L-estimation and compressive sensing," *Signal Processing*, vol. 94, pp. 401–408, January 2014.